POLITECNICO DI TORINO
Repository ISTITUZIONALE

Biobased and Reprocessable Vitrimers Based on Cardanol-Derived Epoxy for More Sustainable Thermosets

Original
Biobased and Reprocessable Vitrimers Based on Cardanol-Derived Epoxy for More Sustainable Thermosets / Albertini, E., Dalle Vacche, S., Bongiovanni, R., Bianco, I., Blengini, G.A., Vitale, A.. - In: ACS SUSTAINABLE CHEMISTRY & ENGINEERING. - ISSN 2168-0485. - 13:5(2025), pp. 2120-2131. [10.1021/acssuschemeng.4c09035]

Availability:
This version is available at: 11583/2997641 since: 2025-03-04T15:06:26Z

Publisher:
American Chemical Society

Published
DOI:10.1021/acssuschemeng.4c09035

Terms of use:

This article is made available under terms and conditions as specified in the corresponding bibliographic description in the repository

Publisher copyright
ACS postprint/Author's Accepted Manuscript

This document is the Accepted Manuscript version of a Published Work that appeared in final form in ACS SUSTAINABLE CHEMISTRY & ENGINEERING, copyright © American Chemical Society after peer review and technical editing by the publisher. To access the final edited and published work see http://dx.doi.org/10.1021/acssuschemeng.4c09035.

(Article begins on next page)

11 November 2026

Bio-based and reprocessable vitrimers based on cardanol-derived epoxy for more sustainable thermosets

Edoardo Albertini[1*], Sara Dalle Vacche[1], Roberta Bongiovanni[1], Isabella Bianco[1], Gian Andrea Blengini[1], Alessandra Vitale[1*]

[1] Politecnico di Torino, Corso Duca degli Abruzzi 24, 10129, Turin, Italy

Abstract

Vitrimers, permanently cross-linked polymers with dynamic covalent bonds that allow the network to change its topology, represent an intriguing field of research as they open new ways of recycling cross-linked polymers, usually not recyclable. The aim of this work is to prepare an innovative bio-based vitrimer starting from the reaction between epoxy and acidic groups. The formulations are thermally cross-linked and then reprocessed by a transesterification reaction. The chemicals used are Cardolite® NC-547, a bio-based epoxy monomer synthetized from cardanol oil, and itaconic acid. Two catalysts are used: 2-ethyl-4-methylimidazole and zinc triflate. The first one mainly takes part in the cross-linking reaction, while the second one has a role in both cross-linking and transesterification reactions. Conversion of 86 % and gel content of 82-84 % are obtained when both the catalysts are used. The thermal reprocessability of the cross-linked polymers is verified by mechanical tests and the properties of the re-processed vitrimers are compared with those of the virgin materials. Results show that a good reprocessability is obtained, with no significant change in conversion and gel content values,

when proper amount of zinc triflate is used. A slight increase in cross-linking density values and mechanical properties is observed after reprocessing. A preliminary Life Cycle Assessment (LCA) is performed with the aim of guiding the research with relevant environmental information. LCA results suggest that bio-based vitrimers could lead to the production of more sustainable products compared to fossil-based ones.

Keywords

Covalent adaptable networks (CANs), transesterification, bio-based epoxy resin, itaconic acid, Life Cycle Assessment, mechanical recycling

1. Introduction

In recent years, plastic consumption has steadily increased, emerging as a major contemporary issue due to its reliance on fossil resources and challenges associated with end-of-life disposal[1]. In particular, thermoset polymers stand out as problematic materials due to difficulties in recycling, negatively impacting the ecosystem[2,3]. Furthermore, thermoset polymers are usually based on epoxies and hardeners with toxicity problems. For example, bisphenol A diglycidyl ether (DGEBA), the most used epoxy resin for high value applications, is produced by reaction of bisphenol A and epichlorohydrin in the presence of sodium hydroxide. Both these precursors are dangerous to human health and the environment[4–6]. Replacement of epoxy resins derived from bisphenol A can certainly lead to products that are safer for human and environmental health. In fact, several epoxy resins from bio-based resources have been synthetized and studied[7–9]. The same concern is directed at the hardeners required for the cross-linking reaction of epoxy resins: amines, anhydrides and organic acids are used as cross-linkers, but they are

usually synthesized from oil and some of them are hazardous to human health. As with their epoxy counterparts, bio-based alternatives to industrial hardeners have been developed[10–12]. Inspired by the twelve principles of green chemistry, a way to solve the end-of-life problem of thermosets is to design recyclable and reformable epoxy resins based on dynamic covalent bonds to form covalent adaptable networks (CANs)[13–15]. CANs are cross-linked polymers that can undergo a reorganization of the network under a proper stimulus (e.g., light, temperature, pressure). This provides the advantages of a network, such as thermal and mechanical resistance, without the permanence of a typical thermoset. CANs can be divided into two main categories depending on the reaction mechanism: dissociative and associative. In the former, a mechanism of network dissociation with loss of network integrity is observed, while the latter exhibit a network rearrangement with a constant cross-linking density[16,17]. Typical CANs systems are the Diels-Alder reaction, transesterification reaction, Shiff-base systems (amino-imine and imine-imine exchange reactions), disulfide exchange, transcarbamoylation and siloxane exchange[18]. In this work we will focus on the transesterification reaction initiated by heat. Based on the seminal work of Leibler et al.[19,20], associative CANs systems based on the transesterification reaction relate to vitrimers. At high temperatures, the viscosity of vitrimers is controlled by chemical exchange reactions, and the thermal viscosity decreases according to Arrhenius law. These materials, like common thermosets, do not dissolve in inert solvents even when heated[17]. In recent years, some work has been published on bio-based vitrimers that combine bio-based epoxy resins with different types of bio-based cross-linkers[21–23].

Cardanol is an unsaturated alkylphenol obtained from cashew nutshell liquid (CNSL). CNSL constitutes 25 % of the weight of nuts and is an important industrial waste product. It is composed of four different meta-alkylphenols differing in the degree of unsaturation of the side chain. Thermal treatment of CNSL, followed by purification, yields industrial grade cardanol[24]. Cardanol can be used as a starting material to synthetize various chemical building blocks for

thermosets, such as epoxy resins and cross-linkers[25–27]. Vitrimers produced from cardanol derivatives have already been studied and applied to 3D printing[28]. In this work Cardolite® NC-547 (NC-547) is selected as epoxy resin due to its high bio-content, i.e. 84 % as declared in the technical datasheet (TDS). Furthermore, the epoxy side groups on the aromatic rings impart good reactivity to the molecule, combined with good flexibility due to the aliphatic side chains, and high flame and organic solvent resistance due to the main aromatic body of the molecule.

The need to combine a bio-based epoxy resin with a bio-based hardener that can undergo a transesterification reaction during reprocessing has led to the emergence of itaconic acid (IA) as cross-linker. IA is a bio-based monounsaturated organic acid, produced from fermentation of sugars by the filamentous fungus *aspergillus terreus,* with a white colour and crystalline structure, and is a viable alternative to acrylic and methacrylic acids[29–32]. In 2004, the U.S. Department of Energy (DOE) inserted IA in the list of the most promising chemical platforms derived from sugars[33]. In this work, IA is used as a cross-linker in combination with two different catalysts.

Imidazoles are used industrially as base catalysts for epoxy-acid reactions, and their reactivity is well known[34–36]. They have also been proposed for the catalysis of transesterification reactions during the reprocessing of vitrimers[37–39], though with very limited efficiency. Instead, zinc complexes (e.g., acetate, trifluoromethanesulfonate, acetylacetonate) are commonly used as catalysts for transesterification[40,41]. Herein, 2-ethyl-4-methylimidazole (EMI-2,4) and zinc trifluoromethanesulfonate (zinc triflate) are used together to catalyse both the cross-linking and the transesterification reactions. In particular, the effect of the content of zinc triflate catalyst is evaluated. Different formulations with various amounts of zinc triflate were cross-linked and characterised by Fourier Transform Infrared spectroscopy in attenuated total reflectance mode (FTIR-ATR), dynamic-mechanical analysis (DMA) and mechanical tests. Gel content and water absorption values were also obtained. Resistance to organic and aqueous solutions was

tested by immersing the samples in various solvents. The reprocessing was performed by hot-pressing ground virgin polymer at high temperature.

To verify the environmental impact of the vitrimer, life-cycle assessment (LCA) was performed, by using ISO standards[42,43] as well as guidelines and reports of the European Commission[44–46] as references. A comparison is made with other systems with non-bio-based reagents to assess whether and to what extent vitrimers may represent an alternative with enhanced environmental performance.

2. Experimental section

2.1 Materials

The synthesized epoxy vitrimer was based on Cardolite® NC-547 (NC-547), a cardanol-based epoxy novolac resin supplied by Cardolite®, with an epoxide equivalent weight of 738 g/eq and a bio-content of 84 %. The chemical structure of NC-547 is showed in Figure 1. Itaconic acid (IA) was used as cross-linker after desiccating in the oven at 80 °C for 30 min. Zinc triflate, $Zn(OTf)_2$, was used as catalyst. When non utilized, IA and $Zn(OTf)_2$ have been stored with desiccant to prevent water absorption. Absolute ethanol was used to dissolve $Zn(OTf)_2$ in order to have good dispersion of the catalyst within the formulation: a 0.062 M ethanol solution was prepared, stored in a refrigerator and used for the preparation of the formulations. 2-ethyl-4-methylimidazole (EMI-2,4) was heated up to 80 °C to melt it before using. IA, $Zn(OTf)_2$, absolute ethanol, EMI-2,4, acetone, toluene, hexane, isopropyl alcohol, as well as hydrochloric acid 37 % and ammonium hydroxide solution ≥ 25 % were purchased from Sigma Aldrich.

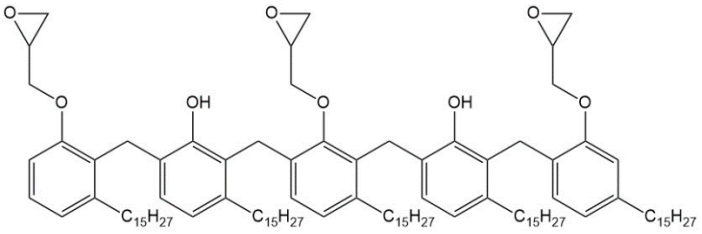

Figure 1 Chemical structure of Cardolite® NC-547

2.2 Preparation and cross-linking of the formulations

For the preparation of the reactive formulations, an equimolar ratio of epoxy/COOH groups (NC-547/IA) was used. 10 mol% (with respect to IA) of the catalyst EMI-2,4 was employed for each formulation. Formulations with different amounts of $Zn(OTf)_2$ (0, 2.5 and 5 mol% with respect to IA) were prepared, in order to study the influence of incorporating a well-known and highly effective catalyst for transesterification into the proposed bio-based epoxy/bio-based hardener system. All components were mixed at room temperature by using a Thinky mixer ARE-250 CE (Thinky Corporation, Japan): a mixing step of 2 min at 2000 rpm, followed by a defoaming step of 1 min at 1500 rpm, was used.

Formulations were thermally cross-linked in silicon molds in an oven (F.lli Galli, Mod. 2100) with the following curing cycle: 2 h at 120 °C, 2 h at 140 °C and 2 h at 150 °C. Such curing cycle was selected based on preliminary results, with the aim of maximizing the esterification yield (based on FTIR conversion data), while minimizing the duration of the process. When not used, formulations were stored in the freezer at -10 °C to prevent any crosslinking during storage.

2.3 V*itrimer reprocessing*

The reprocessing was performed by grinding to fine powder the cross-linked polymers and pressing them for 1 h in a hot press at 180 °C and 130 kN with the help of a 2 mm thick metal mask. The reprocessed materials were grinded and reprocessed for a second time to check the reprocessing repeatability following the same procedure.

2.4 Characterization

FTIR-ATR spectroscopic analysis was performed with Nicolet iS50 spectrometer (ThermoFisher Scientific Inc.) equipped with the universal ATR sampling accessory with a diamond crystal. The spectra were acquired in the 550-4000 cm^{-1} range, with 32 scans per

spectrum and a resolution of 4 cm^{-1}. Conversion (α) at different steps of the cross-linking process was followed by monitoring the decrease of the absorbance of the epoxy groups at 910 cm^{-1} (epoxydic C-O), normalized by the aromatic ring signal at 1580 cm^{-1} (aromatic C=C). Conversion was calculated by Equation 1:

$$\alpha = \left(1 - \frac{\frac{A^{910cm^{-1}}}{A^{1580cm^{-1}}}}{\frac{A_0^{910cm^{-1}}}{A_0^{1580cm^{-1}}}} \right)$$

Equation 1

where A is the area of the absorption peak during the cross-linking process, and A_0 is the area of the peak at time zero (i.e., before the cross-linking process).

Resistance to different solvents was tested by insoluble fraction measurements, performed with acetone, toluene, hexane, isopropyl alcohol, hydrochloric acid 37 % and ammonium hydroxide solution ≥ 25 % as solvent. Samples of ca. 300 mg were cut in small pieces, weighted (m_{0h}), wrapped in a metallic mesh and soaked for 24 h in 10 mL of solvent; they were then dried under the fume hood for 1 night and then in an oven at 80 °C for 2 h, and the residual mass (m_{24h}) of the samples was used to calculate the insoluble fraction by Equation 2:

$$\%\ insoluble = \frac{m_{24h}}{m_{0h}} \times 100$$

Equation 2

Water absorption test was performed to check the amount of water absorbed by cross-linked samples. Samples of ca. 300 mg were weighed (m_{0h}) and soaked in 20 mL of distilled water. After 1 week they were weighed again (m_{1week}) and water absorption was calculated by using Equation 3:

$$\%\ water\ absorption = \frac{m_{1week} - m_{0h}}{m_{0h}} \times 100$$

Equation 3

Zeiss Supra FESEM (Field Emission Scanning Electron Microscopy) with EDX (Energy-Dispersive X-ray) probe using an Oxford liquid-N_2 cooled Si(Li) detector was used to check the morphology and the chemical composition of the samples.

DMA was performed by using Anton Paar Rheometer / Dynamic Mechanical Analyser MCR 702e (Anton Paar, GmbH) equipped with CTD 600 MDR oven and GCU 20-CTD chiller. Tensile tests were performed by varying the temperature from -60 °C to 180 °C at 2 °C/min. The evolution of both the storage modulus (E') and the loss modulus (E'') as a function of temperature was analysed. The maximum of the ratio of E' to E'' (tanδ) was used for calculating the glass transition temperatures (T_g). DMA was also used to determine the cross-linking density ν (moles of cross-linking sites per unit volume, mol/cm^3) by Equation 4[27,47,48]:

$$\nu = \frac{E'_{(80°C)}}{3RT}$$

Equation 4

where E' is the elastic modulus in the rubbery plateau at characteristic temperature (80 °C for our system), R is the gas constant and T is the characteristic temperature in kelvin.

Tensile test machine Z3-X500 (Thumler, GmbH) was used to mechanically characterize the vitrimers before and after reprocessing. Samples of ca. 20 x 10 x 2 mm (l, w, t) were tested with a movement speed of 5 mm/min. Elastic modulus E (calculated between 0 and 0.3 % of deformation) and maximum tensile stress (σ_{max}) were determined.

Thermogravimetric analysis (TGA) was carried out on cross-linked and reprocessed polymers using a Mettler-Toledo TGA 851e Instrument (Columbus, OH, USA), from 25 to 800 °C with a heating rate of 10 °C/min and 50 mL/min of air flow. The curves were normalized to the samples mass.

2.5 Life Cycle Assessment (LCA)

A preliminary LCA was performed with the aim of supporting this research with environmental information and steering future developments towards a more sustainable design of polymeric products. This LCA compares 1 kg of the developed bio-based vitrimer and the same amount of a fossil-based vitrimer. The fossil-based product considered in the LCA is made from a generic epoxy resin and terephthalic acid (TA), replacing NC-547 and IA, respectively. In both cases the epoxy/COOH ratio was kept constant at 1:1 and the amounts of catalysts and ethanol were adjusted accordingly. The system boundaries of the analysis are from-cradle-to-gate, encompassing the processes from raw material extraction to vitrimer production, while the production of specific objects, their use and the end-of-life options are excluded, since the chemical process has not yet been developed.

For the production of the vitrimers, inventory data were collected on a laboratory scale or through stochiometric calculations. Secondary data from literature and Ecoinvent® v3.9.1 (cut-off approach) were employed to represent the production of raw materials. The LCA model was developed with SimaPro 9.5.0.1 software. To align with available literature data for cardanol production, the impacts calculation was performed with the CML-IA baseline method[49], considering the following impact categories: abiotic depletion, abiotic depletion (fossil fuels), global warming potential (GWP 100 years), ozone layer depletion, photochemical oxidation, acidification and eutrophication.

3. Results and discussion

3.1 Vitrimer preparation and characterization

The two main components of the investigated epoxy vitrimers are NC-547 and itaconic acid (IA). The expected curing reaction is illustrated in Figure 2: the epoxy groups of NC-547 react with the carboxylic groups of IA by an esterification reaction (steps (1) and (2) in Figure 2), which can be catalysed by base catalysts (e.g., imidazoles)[50,51]. Etherification and hydrolysis reactions can also occur, as depicted in steps (3) and (4) of Figure 2, respectively. Catalysis of

the esterification reaction by EMI-2,4 imidazole acts on both carboxylic acid and epoxy groups, as shown in Figure 3. In fact, base catalysts are often used to speed up the reaction between carboxyl and epoxy groups through an anionic mechanism, in which the rate of the reaction is controlled by the decomposition of the acid salt formed between the carboxylic group and the catalyst[50,52]. Herein, the amount of EMI-2,4 (i.e., 10 mol%, with respect to IA) was set on the basis of preliminary tests.

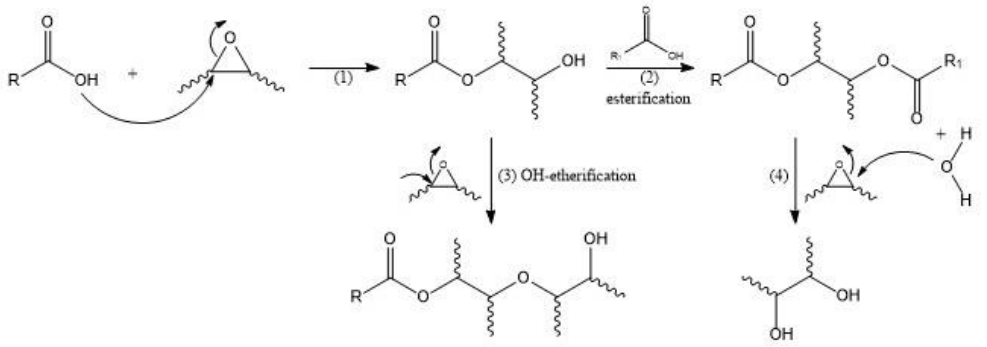

Figure 2 Reaction scheme for carboxylic acid–epoxy system: (1) nucleophilic addition to the epoxy ring; (2) esterification reaction; (3) etherification reaction; (4) hydrolysis reaction

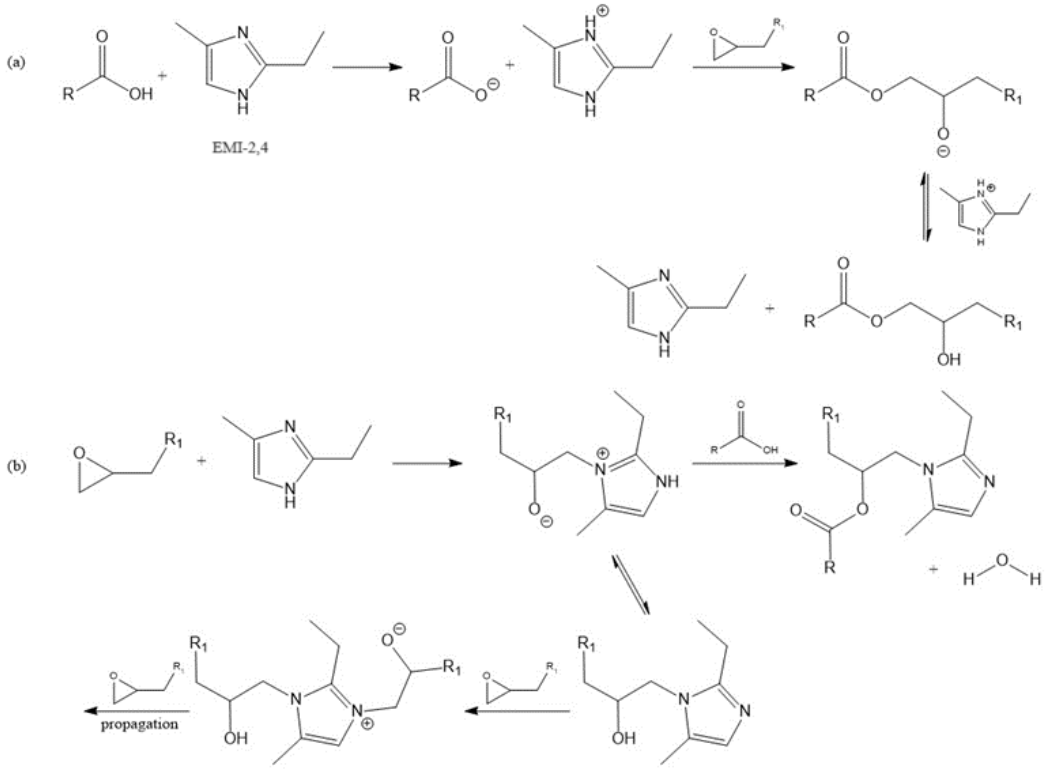

Figure 3 Activation of the esterification reaction by EMI-2,4: a) reaction between carboxylic acid and EMI-2,4; b) reaction between epoxy group and EMI-2,4 (the imidazole remains inside the final structure of the molecule)

In the formulations, zinc triflate was added as catalyst for the transesterification reaction essential for material reprocessing, as described below. However, $Zn(OTf)_2$ also plays an important role in the cross-linking of the starting chemicals. Zn^{2+} acts as a cationic catalyst (Lewis acid) by activating ester carbonyls, stabilizing alkoxide groups, and bringing them into proximity[53,54]. Zn^{2+} catalysts facilitate the cross-linking reaction by coordinating with epoxy groups, enabling their interaction with other epoxy groups[52].

The carboxylic acid–epoxy system was thermally cross-linked through a curing cycle consisting of three steps: 2 h at 120 °C, 2 h at 140 °C and 2 h at 150 °C. The reaction in each step was monitored by FTIR-ATR spectroscopy. Indications in the spectra of the occurrence of the esterification reaction are: decrease of the peak at 910 cm^{-1} due to epoxy groups, appearance of new signals at 1190 cm^{-1} (C-O esters) and at 1720 cm^{-1} (α,β-unsaturated ester), matched by the disappearance of the signals at 1215 cm^{-1} (C-O ethers), at 1685 cm^{-1} (C=O itaconic acid) and at 2500-2800 cm^{-1} (itaconic acid hydrogen bonds). An increase of the β-hydroxyl groups (O-H) signal at 3500 cm^{-1} can also be observed. Furthermore, irreversible side reactions involving carbon double bonds of the aliphatic chains of NC-547 also took place, as attested by the decrease of the bands at 990, 1640 and 3007 cm^{-1}. As an example, FTIR-ATR spectra for the sample with 5 mol% of zinc triflate at the beginning and end of the curing cycle are shown in the Supporting Information (Figure S1).

The conversion of the esterification reaction at the end of each temperature step of the curing cycle was determined by following the decrease of the FTIR-ATR epoxy groups band at 910 cm^{-1}. It is important to note that this signal partially overlaps with the absorption of C-H bonds from double carbon bonds in the aliphatic chains of NC-547 resin. As a result, the epoxy conversion calculated by FTIR is slightly underestimated. The conversion values obtained are presented in Figure 4a-c, showing that all formulations achieved a conversion ≥ 86 % at the end of the curing cycle. The addition of zinc triflate facilitated the reaction at a lower

temperature (120 °C) but resulted in slightly reduced final conversion degrees upon completing the curing cycle. In systems containing 2.5 and 5 mol% of $Zn(OTf)_2$, the cross-linking process was more gradual and homogeneous, leading to defect-free samples with a more uniform morphology (Figure 4d). Notably, no significant difference in the conversion values was observed between samples with 2.5 and 5 mol% of zinc triflate. Conversely, when EMI-2,4 was used alone (sample with 0 mol% of $Zn(OTf)_2$), it appeared to activate the epoxy-acid esterification reaction very abruptly and intensely between 120 °C and 140 °C. Consequently, although the sample with 0 mol% of $Zn(OTf)_2$ exhibited a higher final conversion, it was also characterized by increased fragility and a greater number of macroscopic bubbles (Figure 4d). It is worth emphasizing that the reduction of the activation temperature for the cross-linking reaction attributed to zinc triflate occurs specifically in the presence of the imidazole catalyst. In fact, as shown in Figure S2 of the Supporting Information, at a curing temperature of 120 °C, conversion values of 76 % and 49 % were obtained with a combination of $Zn(OTf)_2$ and EMI-2,4, or $Zn(OTf)_2$ alone, respectively. This finding supports the conclusion, also suggested by the literature, that a synergic catalytic effect arises when zinc triflate and EMI-2,4 are employed together in the same formulation, likely throughout the formation of complexes (see Figure S3 of the Supporting Information)[37,39,55].

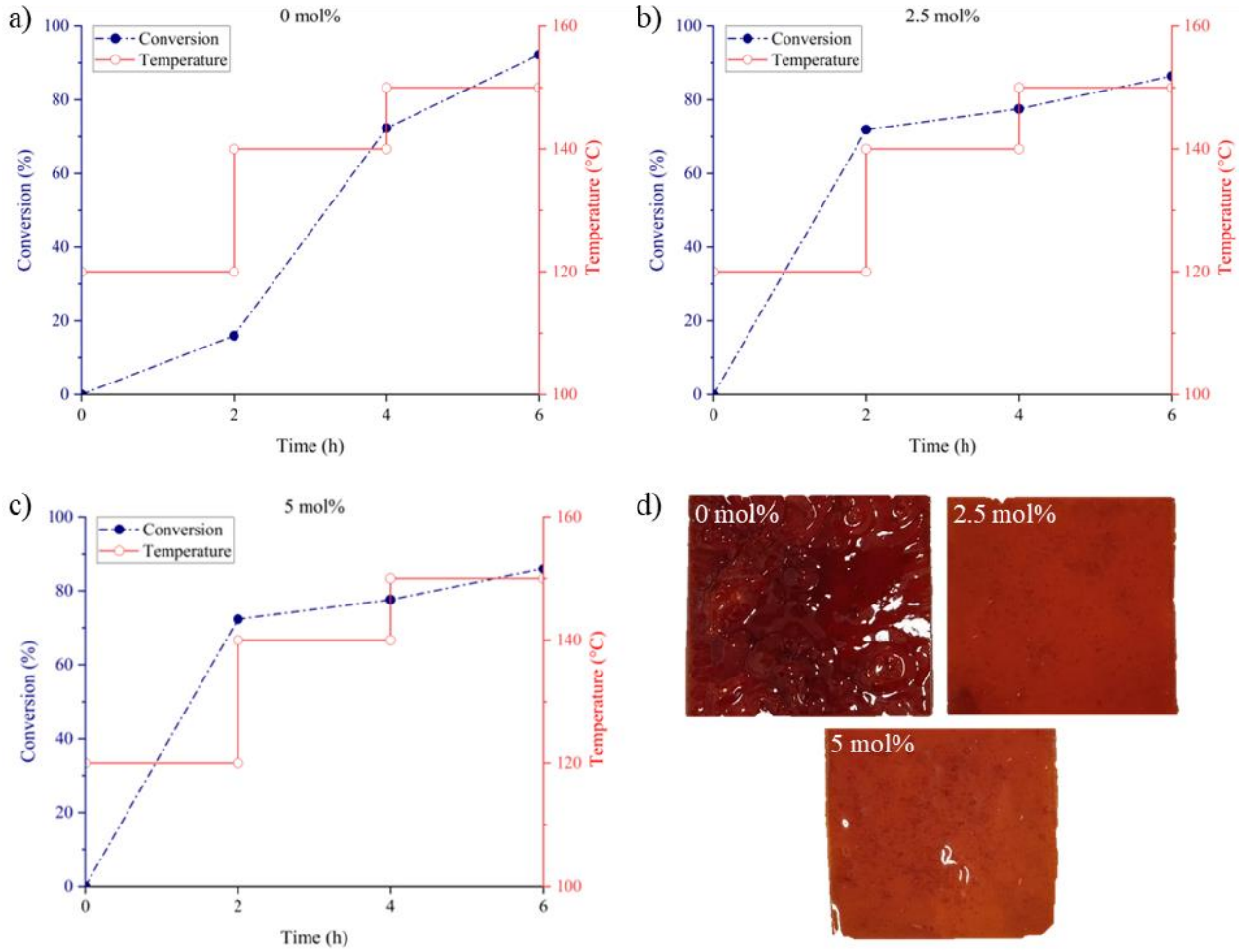

Figure 4 Curing of the vitrimer formulations with different amount of zinc triflate catalyst: conversion values calculated by FTIR-ATR analyses for the formulation with 0 mol% (a), 2.5 mol% (b) and 5 mol% (c) of $Zn(OTf)_2$; digital images of the cured polymers (top view) at the completion of the thermal cycle (d)

FESEM analyses confirmed that the cured vitrimers exhibit a microscopically compact structure and a homogeneous morphology (see Figure S4 in the Supporting Information). FESEM-EDX was used to assess the atomic composition and its uniformity within the samples: both Zn and N were found to be evenly distributed throughout the polymeric matrix, demonstrating the good dispersion of zinc triflate and EMI-2,4 catalysts, respectively. Additionally, the measured Zn content (0 wt.%, 0.08 wt.% and 0.23 wt.%) closely matched the theoretical values (0 wt.%, 0.1 wt.% and 0.2 wt.%).

The insoluble fraction was determined for all the investigated samples (Figure 5a). When acetone was used as solvent, a gel content of approximately 82 % was obtained, with no

significant variation observed by changing the amount of zinc triflate. This indicates that a lower conversion, as seen in systems with 2.5 and 5 mol% of $Zn(OTf)_2$, does not necessarily correlate with a higher soluble fraction or reduced chemical resistance. The comparable insoluble contents obtained for the three samples, despite a different conversion degree, can be attributed to the more uniform chemical structure of vitrimers containing zinc catalyst. This is likely because metal coordination during the cross-linking process leads to a more homogeneous network structure. In contrast, in samples with only EMI-2,4, a part of the reacted epoxy functionalities may form a "micro-gel"-like structure, which remains soluble. Insoluble fraction tests with various organic solvents further supported the improved chemical structure of the samples containing zinc triflate (Figure 5a). In particular, three different organic solvents (toluene, hexane and isopropyl alcohol) were used, each targeting a specific chemical component of NC-547 (i.e., aromatic, aliphatic and polar, respectively; see Figure 1). The most pronounced difference was observed with toluene, where the sample without zinc triflate exhibited higher solubility. This behavior is attributed to the high aromatic content of NC-547 and supports the hypothesis that without zinc, a fraction of cross-linked polymer forms soluble "micro-gels". Conversely, samples with zinc triflate exhibited a more homogeneous cross-linked structure. Also in this case, no differences were observed between samples with varying amounts of zinc triflate. Resistance to acidic and basic aqueous solutions was also evaluated: no weight changes were detected for any sample. Water absorption values (Figure 5b) are similar across all samples, although a slight increase can be observed for the sample containing 5 mol% of zinc triflate, probably due to the hygroscopic nature of zinc triflate.

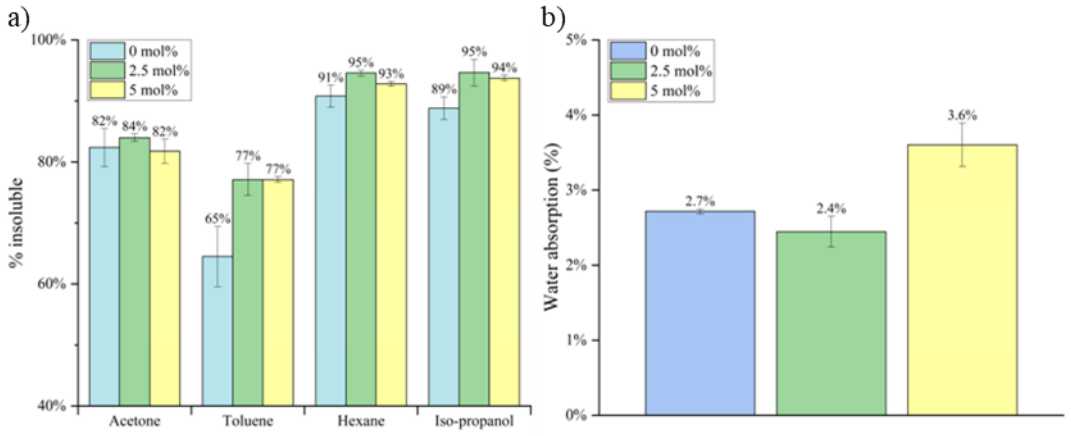

Figure 5 Gel content (a) and water absorption (b) results as a function of the amount of zinc triflate

DMA tests were performed on the cured vitrimers to investigate their thermal and mechanical properties. The results obtained are listed in Table 1, including the T_g (determined as the maximum in the tanδ curves), storage modulus (E'), loss modulus (E'') and cross-linking density (ν). Graphs for E' and tanδ are provided in Figure S5 of the Supporting Information. The T_g values showed minimal variation among the different samples, ranging from 20 to 28 °C. Having a T_g near room temperature, the cured materials are very flexible and rubbery. The cross-linking density values align with those reported in the literature for similar chemical systems[56,57]. However, the calculated values of cross-linking density were slightly lower for the samples containing the zinc catalyst, likely due to the presence of residual ethanol molecules acting as plasticizers (gravimetric analysis revealed that 97 % of ethanol evaporated during the evaporation step). For the same reason, the storage modulus of the sample without zinc triflate is slightly higher (Table 1). Interestingly, increasing the amount of zinc triflate from 2.5 to 5 mol% cross-linking density and storage modulus increase, confirming the efficiency of the combined $Zn(OTf)_2$/EMI-2,4 catalytic system for the epoxy-acid cross-linking reaction.

To summarize, despite their slightly lower conversion value, samples with zinc triflate exhibit a more uniform molecular structure compared to those without it. These samples also demonstrate superior morphology and greater resistance to solvents.

Table 1 DMA results for the three different formulations

$Zn(OTf)_2$ (mol%)	T_g (°C)	$E'_{(80\,°C)}$ (MPa)	$E''_{(80\,°C)}$ (MPa)	ν (mol/cm^3)
0	27	2.71	0.29	3.62×10^{-4}
2.5	20	1.42	0.13	1.61×10^{-4}
5	28	2.17	0.19	2.89×10^{-4}

3.2 Reprocessing of the vitrimers

Reprocessing of the vitrimers was carried out by grinding the cross-linked polymers and hot pressing them with the following parameters: 60 min, 180 °C, 130 kN (see Figure 6). In fact, the developed vitrimers are expected to undergo a transesterification reaction upon heating, as shown in Figure 6b. Zinc triflate can facilitate such reaction by activating carbonyl groups, stabilizing the alkoxide groups and bringing the reacting centers closer together[53,54]. Through this mechanism, zinc actively coordinates with different molecules within the vitrimer promoting an effective reprocessing of the material. Demongeot *et al*. demonstrated how the presence of zinc modifies the chemical environment of C-O and C=O groups in epoxy-acid vitrimers and identified the tetracoordinated form as the most probable[54]. During the transesterification reaction, the type of chemical groups within the network should remain unchanged (Figure 6b). This was confirmed by measuring the epoxy conversion values after the reprocessing, which ranged from 80-82 % for all samples ($\alpha_{0mol\%}$ = 82 %, $\alpha_{2.5mol\%}$ = 82 %, $\alpha_{5mol\%}$ = 80 %). These values are comparable to those obtained before reprocessing, as shown in Figure 4, indicating that no additional reactions occurred between epoxy and carboxylic moieties during the reprocessing step. Gel content tests performed with acetone on the reprocessed samples ($\%gel_{0mol\%}$ = 88 ± 0 %; $\%gel_{2.5mol\%}$ = 84 ± 1 %; $\%gel_{5mol\%}$ = 85 ± 3 %) also produced results consistent with those observed before reprocessing. This confirms that the overall network structure remained largely intact after the reprocessing step.

As shown in Figure 6, the reprocessing of the bio-based vitrimers was successful, with samples containing zinc triflate exhibiting reduced fragility and fewer cracks. Even more interestingly, they displayed fusion lines, which is an indication of the chain mobility typical of vitrimers. In fact, upon exceeding the freezing transition temperature (T_v), covalent bond exchange reactions accelerate, causing vitrimers to behave like a viscoelastic liquid with glass-like fluidity, similar to thermoplastic polymers. T_v is governed by the density of exchangeable cross-links, the exchange reaction kinetics, the mobility of the polymer chains, and the abundance of reactive chemical functions[58]. These findings confirm the vitrimer nature of the samples containing zinc triflate in the original formulation. Conversely, the sample without zinc triflate did not show fusion lines. Despite it is a surprise that the zinc-free sample showed a certain degree of reprocessability, catalyst-free vitrimers relying on transesterification reactions have been previously reported[59]. Furthermore, in this case, it is believed that part of the reprocessability is due to the imidazole, which is known to be a weak transesterification catalyst when used alone[38]. Moreover, it has to be considered that during the thermal reprocessing the double bonds of the cardanol-based resin may undergo oxidation and react at high temperatures through a series of radical oxidative reactions[60].

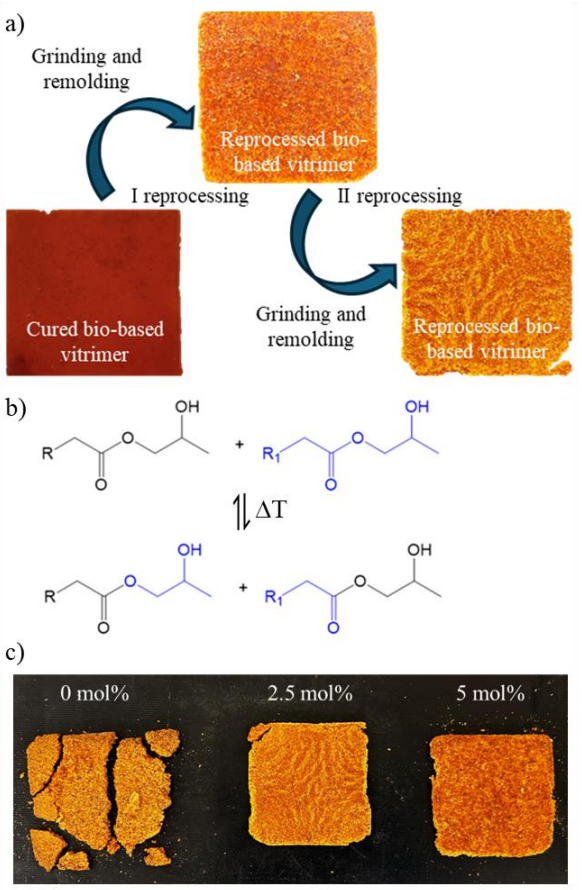

Figure 6 Samples after reprocessing (60 min, 180 °C, 130 kN): a) reprocessing of bio-based vitrimer with 2.5 mol% of zinc triflate; b) transesterification reaction; c) samples after the 2nd reprocessing step

DMA tests on the reprocessed samples revealed a slight increase in both E' and E'', while T_g remained virtually unchanged. Results are reported in Table 2, and the corresponding graphs for E' and tanδ are shown in Figure S6 of the Supporting Information. The modest increase in storage modulus led to a higher cross-linking density, though the values remained comparable to those observed before reprocessing. This increase may be attributed to reactions involving the aliphatic/aromatic double bonds. Overall, the DMA results confirm that the conversion of epoxy groups was unchanged during reprocessing and that minimal secondary reactions occurred. Furthermore, the trends in property values among the different samples were consistent with those observed prior to reprocessing.

Table 2 DMA results for the three different formulations after the 1st and 2nd reprocessing

	$Zn(OTf)_2$ (mol%)	T_g (°C)	$E'_{(80\,°C)}$ (MPa)	$E''_{(80\,°C)}$ (MPa)	ν (mol/cm^3)
1st reprocessing	0	31	3.29	0.28	$3.73x10^{-4}$
	2.5	26	2.56	0.25	$2.90x10^{-4}$
	5	23	2.95	0.25	$3.35x10^{-4}$
2nd reprocessing	0	-	-	-	-
	2.5	28	1.77	0.16	$2.01x10^{-4}$
	5	30	2.73	0.26	$3.10x10^{-4}$

A second reprocessing step was also performed to further demonstrate the effective reprocessability of the investigated system, and thus the robustness and the reproducibility of the proposed process. Samples after the second reprocessing are shown in Figure 6c, while the corresponding graphs for E' and tanδ are provided in Figure S7 of the Supporting Information. The sample without zinc triflate could not be fully reprocessed in the second cycle. Whereas the samples containing 2.5 and 5 mol% of zinc triflate were successfully reprocessed, despite the presence of minor cracks on the edges of the samples due to the use of an open mold during reprocessing. This demonstrates that the combined presence of $Zn(OTf)_2$ and EMI-2,4 catalysts leads to the formation of Zn complexes, which significantly enhance catalytic activity.

After the second reprocessing step, a slight increase in the conversion of epoxy groups was observed ($\alpha_{0mol\%}$ = 93 %, $\alpha_{2.5mol\%}$ = 87 %, $\alpha_{5mol\%}$ = 86 %), indicating the reaction of the remaining available epoxy groups. Gel content tests performed with acetone on the samples after the second reprocessing ($\%gel_{0mol\%}$ = 85 ± 2 %; $\%gel_{2.5mol\%}$ = 86 ± 0 %; $\%gel_{5mol\%}$ = 86 ± 1%) yielded results comparable to those obtained before and after the first reprocessing step, confirming that the overall network structure remained consistent across multiple reprocessing cycles. DMA was performed on the samples from the second reprocessing step and the results are summarized in Table 2. The sample without zinc triflate could not be analyzed due to

extensive cracking (Figure 6c). While the modulus at sub-ambient temperatures was over 50% lower for the samples containing zinc triflate compared to those after the first reprocessing step, the results at room temperature were similar, with a slightly higher T_g observed. Storage module E' at 80 °C decreased by 30 % and 7 % for samples with 2.5 and 5 mol% of zinc triflate, respectively. Correspondingly, the cross-linking density decreased by 27 % and 7 % for the same samples. These findings underscore the critical role of zinc triflate concentration in enabling the reprocessability of the vitrimer system, confirming its importance as a transesterification catalyst.

Tensile tests were conducted to evaluate the mechanical properties of the vitrimers before and after two reprocessing cycles, focusing on the elastic modulus E values. Unfortunately, due to the high number of bubbles, it was not possible to test the sample containing 0 mol% of zinc triflate before reprocessing. The results of the tensile tests are listed in Table 3. Overall, the sample with 5 mol% zinc triflate exhibited a higher modulus compared to the one with 2.5 mol%, aligning the higher cross-linking density observed for this formulation. Following the first reprocessing, a rise in modulus values was observed for both samples. After the second reprocessing, the modulus of the sample with 2.5 mol% zinc triflate further increased, while a slight decrease was observed for the sample with 5 mol%. These changes in modulus values highlight the occurrence of additional chemical reactions during the reprocessing steps in the samples containing zinc triflate.

Table 3 Modulus values before (E^0) and after 1st and 2nd reprocessing steps (E^1 and E^2, respectively)

$Zn(OTf)_2$ (mol%)	0	2.5	5
E^0 (MPa)	-	7.0 ± 0.6	10.7 ± 1.2
E^1 (MPa)	20.7 ± 2.8	10.9 ± 1.2	16.9 ± 2.4
E^2 (MPa)	-	14.2 ± 0.0	14.9 ± 1.0
$T_{5\%}^0$ (°C)	320	320	306

$T_{5\%}^{1}$ (°C)	309	308	312
$T_{5\%}^{2}$ (°C)	295	295	300

Thermogravimetric analysis was performed to check the thermal stability of the samples before and after reprocessing. The thermograms are shown in Figure S8 of the Supporting Information and the results of are listed in Table 3. For all investigated vitrimers, three distinct weight loss events were observed before reprocessing, occurring at approximately 300 °C, 400 °C and 520 °C. The amount of zinc triflate did not alter the thermal degradation onset of the cross-linked resin, as indicated by the similar $T_{5\%}$ values (i.e., the temperature at which 5 % weight loss occurs) reported in Table 3. For samples with 0 and 2.5 mol% zinc triflate, a slight decrease in thermal stability was observed with reprocessing: $T_{5\%}$ decreased by 25 °C following the second reprocessing step (Table 3). In contrast, the sample with 5 mol% of zinc triflate maintained its thermal stability after reprocessing, showing consistent $T_{5\%}$ values and comparable thermograms up to 450 °C before and after reprocessing. For all samples, an increase in the number of reprocessing cycles slowed down the material degradation at high temperature: notably, the final degradation step, occurring at approximately 520 °C, shifted to a higher temperature after the second reprocessing (Figure S8 of the Supporting Information).

3.3 Life Cycle Assessment (LCA) results of bio and fossil-based vitrimer systems

The flow charts in Figure 7 show the LCA model of the two analyzed vitrimer systems, as well as the quantities considered to produce 1 kg of both products.

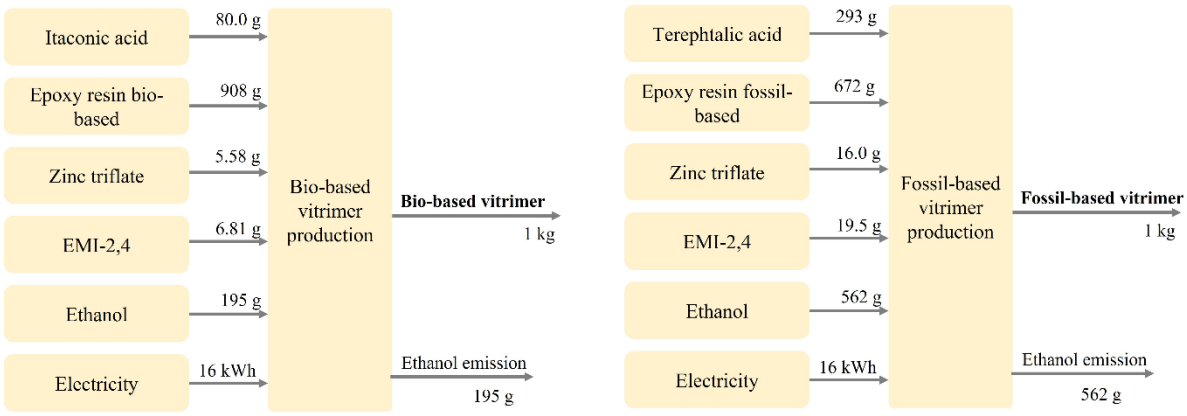

Figure 7 Flow charts of the systems analysed with LCA (left: production of bio-based vitrimer; right: production of fossil-based vitrimer)

The data source for IA production is the study of Robolledo-Leiva et al.[61] The data for the bio-based epoxy resin production is adapted from the Ecoinvent dataset "Epoxy resin, liquid {RER}", but has been modified to include cardanol grade NX-2026 (Cardolite®) as a raw material for the epoxidation reaction step. NX-2026, derived from cashew tree cultivation in China, has publicly available impact data, which were integrated into the LCA model. Since specific datasets for zinc triflate and EMI-2,4 are unavailable in the Ecoinvent database, proxies were employed: zinc oxide and a generic imidazole, respectively. Details of the processes considered in the Ecoinvent® database for both bio-based and fossil-based polymers, along with the corresponding inventory data, are provided in Table S1 of the Supporting Information. Potential impacts for each selected indicator are listed in Table 4. Figure 8 shows a relative comparison of the two products, with the maximum value for each indicator normalized to 100 %. As it can be noticed, across all indicators, the fossil-based vitrimer exhibits higher impacts compared to the bio-based one. The most significant differences are observed in the ozone layer depletion and photochemical oxidation categories, while global warming and acidification impacts are more comparable. The chart also highlights the contribution of involved inputs (materials and energy) and outputs (emissions) to the total impact for each product. Electricity and epoxy resin consistently make substantial contributions across almost all impact categories. In general, impacts associated with IA are slightly higher than those for

TA, but bio-based epoxy resin NC-547 generally has lower impacts than the fossil-based epoxy resin. Additionally, the reduced ethanol requirement in the bio-based solution further lowers its impact compared to the fossil-based alternative. The proxies used in the inventory (zinc oxide and imidazole) show negligible impacts, suggesting that most probably also the zinc triflate and the EMI-2,4 contribute minimally to the final environmental impacts.

Table 4 Environmental impacts result for 1 kg of both vitrimer systems

Impact category	Unit	Bio-based	Fossil-based
Abiotic depletion	kg Sb eq	$4.36x10^{-5}$	$5.64x10^{-5}$
Abiotic depletion (fossil fuels)	MJ	$1.33x10^{2}$	$1.64x10^{2}$
Global warming (GWP100a)	kg CO_2 eq	$1.12x10^{1}$	$1.16x10^{1}$
Ozone layer depletion (ODP)	kg CFC^{-11} eq	$8.39x10^{-7}$	$3.95x10^{-6}$
Photochemical oxidation	kg C_2H_4 eq	$7.98x10^{-2}$	$2.27x10^{-1}$
Acidification	kg SO_2 eq	$4.78x10^{-2}$	$4.83x10^{-2}$
Eutrophication	kg PO_4^{3-} eq	$3.26x10^{-2}$	$3.88x10^{-2}$

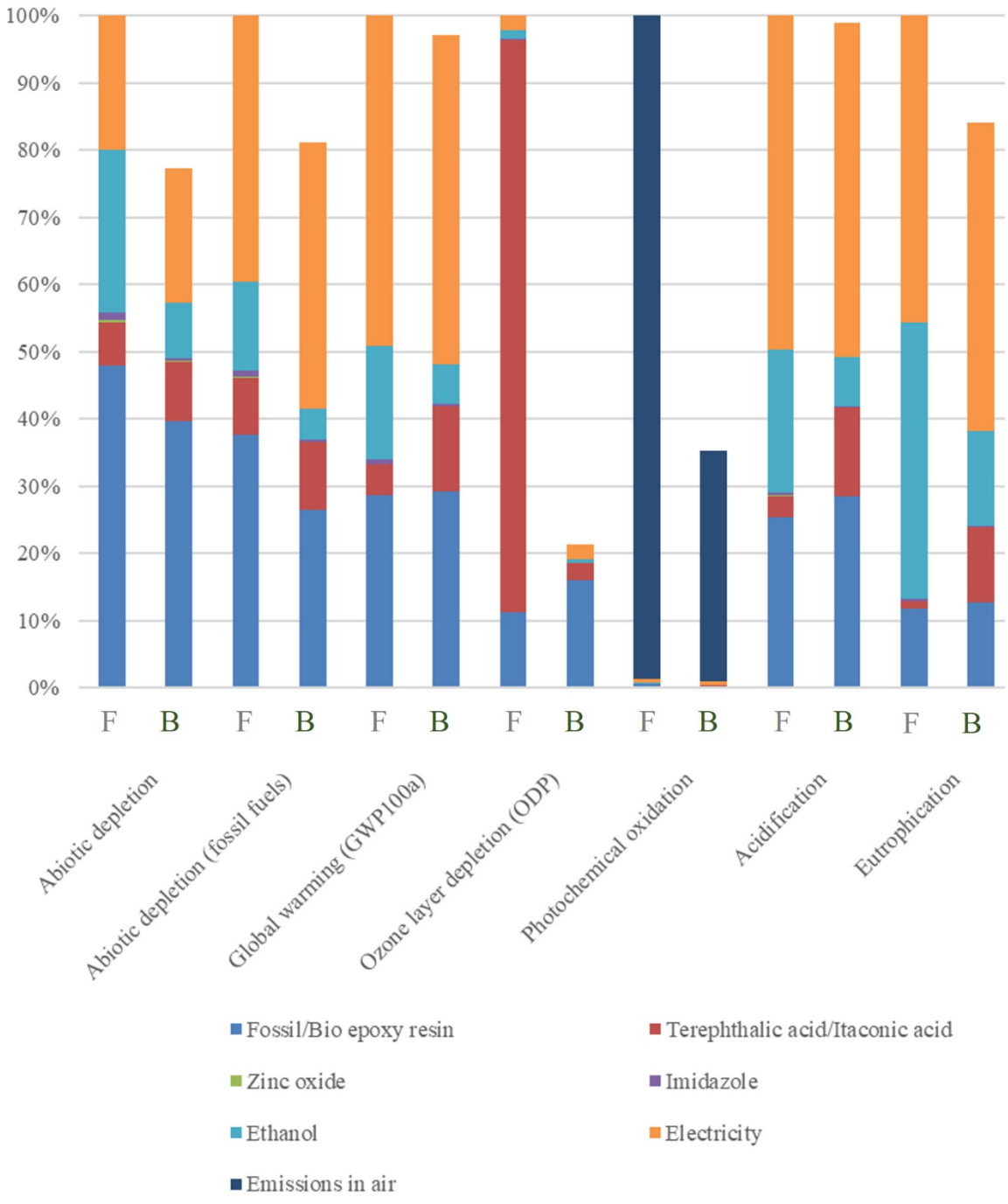

Figure 8 Comparative potential environmental impacts of fossil-based vitrimer (bars indicated with letter F) and bio-based vitrimer (bars indicated with letter B), with contribution analysis of the involved materials, energy and emissions

These preliminary results suggest that the use of a bio-based epoxy resin, following the green chemistry principles and guidelines[62–64], could reduce the environmental impacts of polymeric objects and encourage further research in this field of product design.

In future steps of this research, the described LCA will be fine-tuned to achieve more comprehensive and accurate conclusions. The reported impacts of both vitrimers may currently be overestimated, since the inventory relies on laboratory-scale data. For instance, energy consumption is likely to significantly decrease when scaled up to industrial-scale production, and ethanol emissions could be managed in a more sustainable way. However, it is also possible that products using bio-based resins might exhibit lower mechanical performance, requiring the use of additional material. Consequently, as also highlighted by the European Commission[46], a complete LCA (including the production of a specific product, its use phase and end-of-life considerations) is necessary to evaluate more comprehensively the environmental performance of alternative bio/fossil products.

4. Conclusions

A fully bio-based epoxy vitrimer was successfully synthesized, starting from an epoxy monomer derived from cardanol oil and itaconic acid. The formulations were thermally cross-linked and subsequently reprocessed through a transesterification reaction. Two catalysts were used in the formulations: EMI-2,4 to mainly catalyse the cross-linking reaction and zinc triflate to catalyse both the cross-linking and the transesterification reactions. The influence of the amount of zinc triflate on the cross-linking and re-molding processes was thoroughly investigated. The system demonstrated a degree of reprocessability even without zinc triflate, relying solely on imidazole. However, zinc triflate played a crucial role in achieving successful reprocessing, and its presence was essential for enabling multiple reprocessing cycles of the vitrimer and ensuring effective material recovery. No significant changes were observed in epoxy group conversion (> 80 %), gel content (82-88 %), and cross-linking density (2.0-3.7 x

10^{-4} mol/cm^3) across reprocessing steps, confirming the successful occurrence of the transesterification reaction. Furthermore, the presence of fusion lines after the reprocessing steps with the hot press confirmed the vitrimeric behavior of the system. The thermal reprocessability of the cross-linked polymers was also verified by mechanical tests. When 5 mol% of zinc triflate was used, the elastic modulus increased slightly after reprocessing, rising from 11 MPa after initial cross-linking to 15 MPa following the second reprocessing cycle.

A preliminary LCA was performed to compare the environmental impacts of the investigated bio-based vitrimer (considering the formulation with 2.5 mol% of zinc triflate) with those of a fossil-based vitrimer. Results suggest that the bio-based solution offers significant potential for reducing the environmental footprint of polymeric products, showing lower impacts than its fossil-based counterpart across all analyzed indicators. These results support further research in this direction. Future environmental assessments will align with technological and chemical developments, incorporating prospective LCA to scale-up the processes from laboratory to industrial scale production. They will also consider the complete life cycle of products, including their use phase and end-of-life options.

AKNOWLEDGEMENTS

This study was carried out within the MICS (Made in Italy – Circular and Sustainable) Extended Partnership and received funding from the European Union Next-Generation EU (PIANO NAZIONALE DI RIPRESA E RESILIENZA (PNRR) – MISSIONE 4 COMPONENTE 2, INVESTIMENTO 1.3 – D.D. 1551.11-10-2022, PE00000004). This manuscript reflects only the authors' views and opinions, neither the European Union nor the European Commission can be considered responsible for them.

TOC

Low environmental impact bio-based vitrimers utilizing epoxy and carboxylic acid groups with a dual-catalyst system are developed and successfully reprocessed.

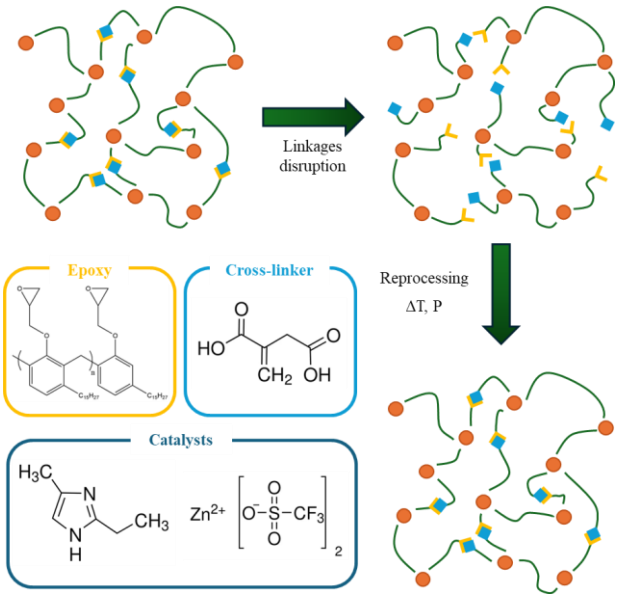

ASSOCIATED CONTENT

Supporting Information. The following files are available free of charge.

Supporting Information (PDF): FTIR spectra of the materials before and after the cross-linking process; conversion values during the thermal cycle for samples with and without EMI-2,4 catalyst; chemical structure of the Zinc complex with triflate and EMI-2,4; FESEM images of samples sections; DMA graphs of the vitrimers before and after reprocessing; TGA thermograms of the vitrimers before and after reprocessing; List of the processes considered in Ecoinvent® database v3.6 for LCA analyses.

AUTHOR INFORMATION

Corresponding Authors

* edoardo.albertini@polito.it (EA)

* alessandra.vitale@polito.it (AV)

REFERENCES

(1) Walker, T. R.; Fequet, L. Current Trends of Unsustainable Plastic Production and Micro(Nano)Plastic Pollution. *Trends in Analytical Chemistry* **2023**, *160*, 1–7. https://doi.org/10.1016/j.trac.2023.116984.

(2) Memon, H.; Wei, Y.; Zhu, C. Recyclable and Reformable Epoxy Resins Based on Dynamic Covalent Bonds – Present, Past, and Future. *Polym Test* **2022**, *105*, 1–20. https://doi.org/10.1016/j.polymertesting.2021.107420.

(3) Dinu, R.; Lafont, U.; Damiano, O.; Mija, A. Sustainable and Recyclable Thermosets with Performances for High Technology Sectors. An Environmental Friendly Alternative to Toxic Derivatives. *Front Mater* **2023**, *10:1242507*, 1–11. https://doi.org/10.3389/fmats.2023.1242507.

(4) Okada, H.; Tokunaga, T.; Liu, X.; Takayanagi, S.; Matsushima, A.; Shimohigashi, Y. Direct Evidence Revealing Structural Elements Essential for the High Binding Ability of Bisphenol a to Human Estrogen-Related Receptor-γ. *Environ Health Perspect* **2008**, *116* (1), 32–38. https://doi.org/10.1289/ehp.10587.

(5) Auvergne, R.; Caillol, S.; David, G.; Boutevin, B.; Pascault, J. P. Biobased Thermosetting Epoxy: Present and Future. *Chem Rev* **2014**, *114* (2), 1082–1115. https://doi.org/10.1021/cr3001274.

(6) vom Saal, F. S.; Hughes, C. An Extensive New Literature Concerning Low-Dose Effects of Bisphenol A Shows the Need for a New Risk Assessment. *Environ Health Perspect* **2005**, *113* (8), 926–933. https://doi.org/10.1289/ehp.7713.

(7) Ares-Elejoste, P.; Seoane-Rivero, R.; Gandarias, I.; Iturmendi, A.; Gondra, K. Sustainable Alternatives for the Development of Thermoset Composites with Low Environmental Impact. *Polymers (Basel)* **2023**, *15, 2939* (13), 1–16. https://doi.org/10.3390/polym15132939.

(8) Nikafshar, S.; Zabihi, O.; Hamidi, S.; Moradi, Y.; Barzegar, S.; Ahmadi, M.; Naebe, M. A Renewable Bio-Based Epoxy Resin with Improved Mechanical Performance That Can Compete with DGEBA. *RSC Adv* **2017**, *7* (14), 8694–8701. https://doi.org/10.1039/c6ra27283e.

(9) Faye, I.; Decostanzi, M.; Ecochard, Y.; Caillol, S. Eugenol Bio-Based Epoxy Thermosets: From Cloves to Applied Materials. *Green Chemistry* **2017**, *19* (21), 5236–5242. https://doi.org/10.1039/c7gc02322g.

(10) Fache, M.; Darroman, E.; Besse, V.; Auvergne, R.; Caillol, S.; Boutevin, B. Vanillin, a Promising Biobased Building-Block for Monomer Synthesis. *Green Chemistry* **2014**, *16* (4), 1987–1998. https://doi.org/10.1039/c3gc42613k.

(11) Ismail, T. N. M. T.; Hassan, H. A.; Hirose, S.; Taguchi, Y.; Hatakeyama, T.; Hatakeyama, H. Synthesis and Thermal Properties of Ester-Type Crosslinked Epoxy Resins Derived from Lignosulfonate and Glycerol. *Polym Int* **2010**, *59* (2), 181–186. https://doi.org/10.1002/pi.2705.

(12) Darroman, E.; Bonnot, L.; Auvergne, R.; Boutevin, B.; Caillol, S. New Aromatic Amine Based on Cardanol Giving New Biobased Epoxy Networks with Cardanol. *European Journal of Lipid Science and Technology* **2015**, *117* (2), 178–189. https://doi.org/10.1002/ejlt.201400248.

(13) Bowman, C. N.; Kloxin, C. J. Covalent Adaptable Networks: Reversible Bond Structures Incorporated in Polymer Networks. *Angewandte Chemie - International Edition* **2012**, *51* (18), 4272–4274. https://doi.org/10.1002/anie.201200708.

(14) Kloxin, C. J.; Scott, T. F.; Adzima, B. J.; Bowman, C. N. Covalent Adaptable Networks (CANs): A Unique Paradigm in Cross-Linked Polymers. *Macromolecules* **2010**, *43* (6), 2643–2653. https://doi.org/10.1021/ma902596s.

(15) Kloxin, C. J.; Bowman, C. N. Covalent Adaptable Networks: Smart, Reconfigurable and Responsive Network Systems. *Chem Soc Rev* **2013**, *42* (17), 7161–7173. https://doi.org/10.1039/c3cs60046g.
(16) Abdur Rashid, M.; Liu, W.; Wei, Y.; Jiang, Q. Review of Reversible Dynamic Bonds Containing Intrinsically Flame Retardant Biomass Thermosets. *Eur Polym J* **2022**, *173*, 1–17. https://doi.org/10.1016/j.eurpolymj.2022.111263.
(17) Denissen, W.; Winne, J. M.; Du Prez, F. E. Vitrimers: Permanent Organic Networks with Glass-like Fluidity. *Chem Sci* **2016**, *7* (1), 30–38. https://doi.org/10.1039/c5sc02223a.
(18) Schenk, V.; Labastie, K.; Destarac, M.; Olivier, P.; Guerre, M. Vitrimer Composites: Current Status and Future Challenges. *Mater Adv* **2022**, *3* (22), 8012–8029. https://doi.org/10.1039/d2ma00654e.
(19) Capelot, M.; Unterlass, M. M.; Tournilhac, F.; Leibler, L. Catalytic Control of the Vitrimer Glass Transition. *ACS Macro Lett* **2012**, *1* (7), 789–792. https://doi.org/10.1021/mz300239f.
(20) Capelot, M.; Montarnal, D.; Tournilhac, F.; Leibler, L. Metal-Catalyzed Transesterification for Healing and Assembling of Thermosets. *J Am Chem Soc* **2012**, *134* (18), 7664–7667. https://doi.org/10.1021/ja302894k.
(21) Guggari, S.; Magliozzi, F.; Malburet, S.; Graillot, A.; Destarac, M.; Guerre, M. Vanillin-Based Epoxy Vitrimers: Looking at the Cystamine Hardener from a Different Perspective. *ACS Sustain Chem Eng* **2023**, *11* (15), 6021–6031. https://doi.org/10.1021/acssuschemeng.3c00379.
(22) Hong, J.; Hong, Y.; Jeong, J.; Oh, D.; Goh, M. Robust Biobased Vitrimers and Its Application to Closed-Loop Recyclable Carbon Fiber-Reinforced Composites. *ACS Sustain Chem Eng* **2023**, *11* (38), 14112–14123. https://doi.org/10.1021/acssuschemeng.3c03468.
(23) Verdugo, P.; Santiago, D.; De la Flor, S.; Serra, À. A Biobased Epoxy Vitrimer with Dual Relaxation Mechanism: A Promising Material for Renewable, Reusable, and Recyclable Adhesives and Composites. *ACS Sustain Chem Eng* **2024**, *12* (15), 5965–5978. https://doi.org/10.1021/acssuschemeng.4c00205.
(24) Fouquet, T.; Puchot, L.; Verge, P.; Bomfim, J. A. S.; Ruch, D. Exploration of Cardanol-Based Phenolated and Epoxidized Resins by Size Exclusion Chromatography and MALDI Mass Spectrometry. *Anal Chim Acta* **2014**, *843*, 46–58. https://doi.org/10.1016/j.aca.2014.07.030.
(25) Voirin, C.; Caillol, S.; Sadavarte, N. V.; Tawade, B. V.; Boutevin, B.; Wadgaonkar, P. P. Functionalization of Cardanol: Towards Biobased Polymers and Additives. *Polym Chem* **2014**, *5* (9), 3142–3162. https://doi.org/10.1039/c3py01194a.
(26) Kinaci, E.; Can, E.; La Scala, J. J.; Palmese, G. R. Influence of Epoxidized Cardanol Functionality and Reactivity on Network Formation and Properties. *Polymers (Basel)* **2020**, *12* (9), 1–14. https://doi.org/10.3390/polym12091956.
(27) Jaillet, F.; Darroman, E.; Ratsimihety, A.; Auvergne, R.; Boutevin, B.; Caillol, S. New Biobased Epoxy Materials from Cardanol. *European Journal of Lipid Science and Technology* **2014**, *116* (1), 63–73. https://doi.org/10.1002/ejlt.201300193.
(28) Capannelli, J. M.; Dalle Vacche, S.; Vitale, A.; Bouzidi, K.; Beneventi, D.; Bongiovanni, R. A Biobased Epoxy Vitrimer/Cellulose Composite for 3D Printing by Liquid Deposition Modelling. *Polym Test* **2023**, *127*, 108172. https://doi.org/10.1016/j.polymertesting.2023.108172.
(29) Devi, N.; Singh, S.; Manickam, S.; Cruz-Martins, N.; Kumar, V.; Verma, R.; Kumar, D. Itaconic Acid and Its Applications for Textile, Pharma and Agro-Industrial

Purposes. *Sustainability (Switzerland)*. MDPI October 24, 2022. https://doi.org/10.3390/su142113777.
(30) Teleky, B. E.; Vodnar, D. C. Recent Advances in Biotechnological Itaconic Acid Production, and Application for a Sustainable Approach. *Polymers (Basel)* **2021**, *13* (20), 1–22. https://doi.org/10.3390/polym13203574.
(31) Chang, P. C.; Hsu, H. Y.; Jang, G. W. Biological Routes to Itaconic and Succinic Acids. *Physical Sciences Reviews* **2016**, *1* (8), 1–17. https://doi.org/10.1515/psr-2016-0052.
(32) Pomraning, K. R.; Dai, Z.; Munoz, N.; Kim, Y. M.; Gao, Y.; Deng, S.; Lemmon, T.; Swita, M. S.; Zucker, J. D.; Kim, J.; Mondo, S. J.; Panisko, E.; Burnet, M. C.; Webb-Robertson, B. J. M.; Hofstad, B.; Baker, S. E.; Burnum-Johnson, K. E.; Magnuson, J. K. Itaconic Acid Production Is Regulated by LaeA in Aspergillus Pseudoterreus. *Metab Eng Commun* **2022**, *15*, 1–14. https://doi.org/10.1016/j.mec.2022.e00203.
(33) Program, B.; Werpy, T.; Petersen, G. *Top Value Added Chemicals from Biomass Volume I-Results of Screening for Potential Candidates from Sugars and Synthesis Gas*. https://www.osti.gov/biblio/15008859 (accessed 2025-01-09), U.S. Department of Energy – Technical Report.
(34) Jin, J.-I.; Choi, E.-J.; Ryu, S.-C.; Lenz, R. W.; Ober, C. K.; Luise, R. R. U.; Blackwell, J.; Cheng, H.-M. Curing Mechanism and Thermal Properties of Epoxy-Imidazole Systems. *Biswas, A. Macromolecules* **1989**, *22* (8), 99–104.
(35) Ding, X. M.; Chen, L.; Guo, D. M.; Liu, B. W.; Luo, X.; Lei, Y. F.; Zhong, H. Y.; Wang, Y. Z. Controlling Cross-Linking Networks with Different Imidazole Accelerators toward High-Performance Epoxidized Soybean Oil-Based Thermosets. *ACS Sustain Chem Eng* **2021**, *9* (8), 3267–3277. https://doi.org/10.1021/acssuschemeng.0c08852.
(36) Morinaga, H.; Sakamoto, M. Co-Cross-Linking of Bio-Based Multi-Functional Epoxide and Bisphenol A Diglycidyl Ether with 2-Ethyl-4-Methylimidazole. *Tetrahedron Lett* **2018**, *59* (43), 3889–3891. https://doi.org/10.1016/j.tetlet.2018.09.036.
(37) Nakatake, D.; Yazaki, R.; Matsushima, Y.; Ohshima, T. Transesterification Reactions Catalyzed by a Recyclable Heterogeneous Zinc/Imidazole Catalyst. *Adv Synth Catal* **2016**, *358* (15), 2569–2574. https://doi.org/10.1002/adsc.201600229.
(38) Falireas, P. G.; Thomassin, J. M.; Debuigne, A. Imidazolium-Catalyzed Dynamic Ester Cross-Links towards Reprocessable Epoxy Vitrimers. *Eur Polym J* **2021**, *147*, 1–10. https://doi.org/10.1016/j.eurpolymj.2021.110296.
(39) Casado, J.; Konuray, O.; Roig, A.; Fernández-Francos, X.; Ramis, X. 3D Printable Hybrid Acrylate-Epoxy Dynamic Networks. *Eur Polym J* **2022**, *173*, 1–12. https://doi.org/10.1016/j.eurpolymj.2022.111256.
(40) Niu, X.; Wang, F.; Li, X.; Zhang, R.; Wu, Q.; Sun, P. Using Zn2+ Ionomer to Catalyze Transesterification Reaction in Epoxy Vitrimer. *Ind Eng Chem Res* **2019**, *58* (14), 5698–5706. https://doi.org/10.1021/acs.iecr.9b00090.
(41) Esposito, R.; Melchiorre, M.; Annunziata, A.; Cucciolito, M. E.; Ruffo, F. Emerging Catalysis in Biomass Valorisation: Simple Zn(II) Catalysts for Fatty Acids Esterification and Transesterification. *ChemCatChem* **2020**, *12* (23), 5858–5879. https://doi.org/10.1002/cctc.202001144.
(42) ISO International Standard. *Environmental Management - Life Cycle Assessment - Requirements and Guidelines*; ISO 14044:2006/Amd2:2020. Vol. 14044. ISO, 2020.
(43) ISO International Standard. *Environmental Management - Life Cycle Assessment - Principles and Framework*; ISO 14040:2006/Amd1:2020. Vol. 14040. ISO, 2020.

(44) Manfredi, S.; Allacker, K.; Chomkhamsri, K.; Pelletier, N.; Maia De Souza, D. *Product Environmental Footprint (PEF) Guide*; Ares(2012)873782; European Commission - Joint Research Centre: Ispra, Italy, 2012. https://www.reteclima.it/wp-content/uploads/PEF-methodology-final-draft.pdf (accessed 2025-01-09)
(45) Wolf, M.-Andree.; Pant, Rana.; Chomkhamsri, Kirana.; Sala, Serenella.; Pennington, David. *The International Reference Life Cycle Data System (ILCD) Handbook*; JRC Reference Report; European Commission - Joint Research Centre: Luxembourg, 2012. https://doi.org/10.2788/85727.
(46) Caldeira, C.; Farcal, L. R.; Garmendia Aguirre, I.; Mancini, L.; Tosches, D.; Amelio, A.; Rasmussen, K.; Rauscher, H.; Riego Sintes, J.; Sala, S. *Safe and Sustainable by Design Chemicals and Materials - Framework for the Definition of Criteria and Evaluation Procedure for Chemicals and Materials*; JRC Technical Report; European Commission - Joint Research Centre: Luxembourg, 2022. https://doi.org/10.2760/487955.
(47) Azcune, I.; Huegun, A.; Ruiz de Luzuriaga, A.; Saiz, E.; Rekondo, A. The Effect of Matrix on Shape Properties of Aromatic Disulfide Based Epoxy Vitrimers. *Eur Polym J* **2021**, *148*, 1–10. https://doi.org/10.1016/j.eurpolymj.2021.110362.
(48) Memon, H.; Wei, Y.; Zhu, C. Correlating the Thermomechanical Properties of a Novel Bio-Based Epoxy Vitrimer with Its Crosslink Density. *Mater Today Commun* **2021**, *29*, 1–7. https://doi.org/10.1016/j.mtcomm.2021.102814.
(49) de Bruijn, H.; van Duin, R.; Huijbregts, M. A. J.; Guinée, J. B.; Gorree, M.; Heijungs, R.; Huppes, G.; Kleijn, R.; Koning, A.; Oers, L.; Wegener Sleeswijk, A.; Suh, S.; Udo de Haes, H. A. *Handbook on Life Cycle Assessment - Operational Guide to the ISO Standards*; Kluwer Academic Publishers, 2002; Vol. 7.
(50) Vidil, T.; Tournilhac, F.; Musso, S.; Robisson, A.; Leibler, L. Control of Reactions and Network Structures of Epoxy Thermosets. *Prog Polym Sci* **2016**, *62*, 126–179. https://doi.org/10.1016/j.progpolymsci.2016.06.003.
(51) Pire, M.; Norvez, S.; Iliopoulos, I.; Le Rossignol, B.; Leibler, L. Imidazole-Promoted Acceleration of Crosslinking in Epoxidized Natural Rubber/Dicarboxylic Acid Blends. *Polymer (Guildf)* **2011**, *52* (23), 5243–5249. https://doi.org/10.1016/j.polymer.2011.09.032.
(52) Blank, W. J.; He, Z. A.; Picci, M. Catalysis of the Epoxy-Carboxyl Reaction. *Journal of Coatings Technology* **2002**, *74* (926), 33–41. https://doi.org/10.1007/BF02720158.
(53) Fang, M.; Liu, X.; Feng, Y.; Lu, B.; Huang, M.; Liu, C.; Shen, C. Influence of Zn2+ Catalyst Stoichiometry on Curing Dynamics and Stress Relaxation of Polyester-Based Epoxy Vitrimer. *Polymer (Guildf)* **2023**, *278*, 1–8. https://doi.org/10.1016/j.polymer.2023.126010.
(54) Demongeot, A.; Mougnier, S. J.; Okada, S.; Soulié-Ziakovic, C.; Tournilhac, F. Coordination and Catalysis of Zn2+ in Epoxy-Based Vitrimers. *Polym Chem* **2016**, *7* (27), 4486–4493. https://doi.org/10.1039/c6py00752j.
(55) Tašner, M.; Vušak, D.; Kekez, I.; Gabud, A.; Pilepić, V.; Mrvoš-Sermek, D.; Matković-Čalogović, D. Zn(II) Halide Coordination Compounds with Imidazole and 2-Methylimidazole. Structural and Computational Characterization of Intermolecular Interactions and Disorder. *Heliyon* **2022**, *8* (10), 1–11. https://doi.org/10.1016/j.heliyon.2022.e11100.
(56) Ecochard, Y.; Decostanzi, M.; Negrell, C.; Sonnier, R.; Caillol, S. Cardanol and Eugenol Based Flame Retardant Epoxy Monomers for Thermostable Networks. *Molecules* **2019**, *24* (9), 1–21. https://doi.org/10.3390/molecules24091818.
(57) Manarin, E.; Corsini, F.; Trano, S.; Fagiolari, L.; Amici, J.; Francia, C.; Bodoardo, S.; Turri, S.; Bella, F.; Griffini, G. Cardanol-Derived Epoxy Resins as Biobased Gel

Polymer Electrolytes for Potassium-Ion Conduction. *ACS Appl Polym Mater* **2022**, *4* (5), 3855–3865. https://doi.org/10.1021/acsapm.2c00335.
(58) Kaiser, S.; Novak, P.; Giebler, M.; Gschwandl, M.; Novak, P.; Pilz, G.; Morak, M.; Schlögl, S. The Crucial Role of External Force in the Estimation of the Topology Freezing Transition Temperature of Vitrimers by Elongational Creep Measurements. *Polymer (Guildf)* **2020**, *204*, 1–9. https://doi.org/10.1016/j.polymer.2020.122804.
(59) Zhu, Y.; Li, W.; He, Z.; Zhang, K.; Nie, X.; Fu, R.; Chen, J. Catalyst-Free Cardanol-Based Epoxy Vitrimers for Self-Healing, Shape Memory, and Recyclable Materials. *Polymers (Basel)* **2024**, *16* (3), 1–14. https://doi.org/10.3390/polym16030307.
(60) DePolo, G.; Iedema, P.; Shull, K.; Hermans, J. Comprehensive Characterization of Drying Oil Oxidation and Polymerization Using Time-Resolved Infrared Spectroscopy. *Macromolecules* **2024**, *57* (17), 8263–8276. https://doi.org/10.1021/acs.macromol.4c01164.
(61) Rebolledo-Leiva, R.; Moreira, M. T.; González-García, S. Environmental Assessment of the Production of Itaconic Acid from Wheat Straw under a Biorefinery Approach. *Bioresour Technol* **2022**, *345*, 1–9. https://doi.org/10.1016/j.biortech.2021.126481.
(62) Anastas, P.; Eghbali, N. Green Chemistry: Principles and Practice. *Chem Soc Rev* **2010**, *39* (1), 301–312. https://doi.org/10.1039/b918763b.
(63) Anastas, P. T.; Warner, J. C. *Green Chemistry: Theory and Practice*; Oxford University Press: Oxford, 2000. https://doi.org/10.1093/oso/9780198506980.001.0001.
(64) Chen, T. L.; Kim, H.; Pan, S. Y.; Tseng, P. C.; Lin, Y. P.; Chiang, P. C. Implementation of Green Chemistry Principles in Circular Economy System towards Sustainable Development Goals: Challenges and Perspectives. *Science of the Total Environment* **2020**, *716*, 1–16. https://doi.org/10.1016/j.scitotenv.2020.136998.